INTERNATIONAL JOURNAL OF HYDROGEN ENERGY XXX (2015) 1–8

Available online at www.sciencedirect.com

ScienceDirect

journal homepage: www.elsevier.com/locate/he

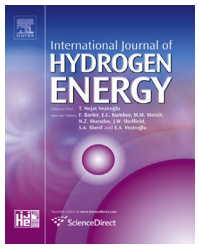

# High surface area coatings for hydrogen evolution cathodes prepared by magnetron sputtering

*Xiaoling Zhang* [a,**], *Joanne Hampshire* [a], *Kevin Cooke* [a], *Xiaohong Li* [b,*], *Derek Pletcher* [c], *Shaun Wright* [d], *Kristian Hyde* [d]

[a] *Teer Coatings Ltd, Miba Coating Group, West Stone House, Berry Hill Industrial Estate, Droitwich Spa, Worcestershire WR9 9AS, UK*

[b] *Renewable Energy Group, College of Engineering, Mathematics and Physical Sciences, University of Exeter, TR10 9FE, UK*

[c] *School of Chemistry, University of Southampton, Southampton SO17 1BJ, UK*

[d] *ITM Power, 22 Atlas Way, Sheffield S4 7QQ, UK*

ARTICLE INFO

*Article history:*
Received 17 October 2014
Received in revised form
18 December 2014
Accepted 24 December 2014
Available online xxx

*Keywords:*
Magnetron sputtering
High surface area coatings
Catalyst coatings
Water electrolysis

ABSTRACT

A novel magnetron sputtering technique is described for the deposition of durable, high surface area metal and alloy deposits (thickness up to several microns) onto nickel and steel substrates. The materials deposited include platinum, nickel, nickel alloys and steels. The structure of the deposits is characterised and it is demonstrated that some high surface area coatings are efficient and effective electrocatalysts for hydrogen evolution in alkaline media and coated mesh electrodes have been tested in a modern water electrolyser configuration.



## Introduction

High area electrode surfaces have an important role in modern electrochemical technology [1–3] since they allow performance goals to be achieved with lower energy consumption. This is particularly the case with energy intensive processes such as the chlor-alkali process and water electrolysis. Water electrolysis is one route to hydrogen production and hydrogen is predicted to have an increasing role as a fuel and energy storage medium in green energy economies [4,5]. There are substantial advantages in employing an alkaline electrolyte for water electrolysis and there are great opportunities for the development of non-precious metal electrocatalysts for both hydrogen and oxygen evolution [6]. Such electrodes must be low cost, stable in the cell operating conditions, robust and operate at high current densities with a low overpotential. High area nickel, nickel alloys and steels are candidates for such applications [6–12].

Similar to other Physical Vapour Deposition (PVD) processes, magnetron sputtering is fundamentally an environmentally benign process [13–17]. It requires no hazardous

* *Corresponding author*. Tel.: +44 (0)1326 255769; fax: +44 (0)1326 371859.
** *Corresponding author*.
E-mail addresses: xiaoling.zhang@miba.com (X. Zhang), X.Li@exeter.ac.uk (X. Li).

http://dx.doi.org/10.1016/j.ijhydene.2014.12.107

**Table 1 – Comparison of the compositions of the deposits with those of the magnetron targets. Target compositions are taken from specification. % compositions of the deposits are determined by EDAX.**

| Element | Ni80Cr20 | | Monel 400 | | Hastelloy C276 | | Hastelloy C22 | |
|---|---|---|---|---|---|---|---|---|
| | Target | Deposit | Target | Deposit | Target | Deposit | Target | Deposit |
| Cr | 20.0 | 21.5 | | | 16.0 | 16.5 | 22.0 | 21.5 |
| Ni | 80.0 | 78.5 | 65.0 | 65.5 | 55.5 | 53.5 | 56.0 | 52.5 |
| Fe | | | 2.0 | 5.0 | 7.0 | 7.5 | 3.0 | 5.0 |
| Cu | | | 33.0 | 29.5 | | | | |
| Mn | | | | | | | | |
| Mo | | | | | 18.0 | 18.5 | 13.5 | 16.5 |
| W | | | | | 3.5 | 4.0 | 3.0 | 3.0 |
| Co | | | | | | | 2.5 | 1.5 |
| Thickness | | 1.5 μm | | 1.4 μm | | 1.5 μm | | 1.5 μm |

liquids or toxic/flammable materials and there are no noxious by-products which could result in air pollution or hazardous waste. This contrasts strongly with other common deposition processes such as Chemical Vapour Deposition (CVD), spraying and electroplating [18–20]. In addition, magnetron sputtering can lead to coatings with controlled and variable composition, good adhesion, crystalline structure, controlled, variable and uniform thickness [13–17] and such coatings can be achieved with a wide range of both substrates (metal, polymer, carbon cloth, glass, rubber, ceramics and wood in various forms including flat surfaces, meshes, powders, fibres and particles) and depositing materials (metals, alloys, oxides, nitrides and carbides as well as multilayered structures or mixtures) [21,22]. It is therefore well-suited to the fabrication of electrode coatings.

In this paper, a novel magnetron sputtering technique is described that allows the deposition of typically micron thick coatings with significantly increased surface areas. The details of deposition method and conditions refer to a recently published patent [23]. Metallic and alloy high surface area coatings (HSACs) have been achieved by changing the arrangement of the deposition system and the deposition parameters, including: magnetron configuration, working gases, deposition pressure, and the sputtering power. The advantage of this approach is illustrated by the preparation of coated nickel and steel meshes with coatings that are appropriate for high performance, hydrogen evolution cathodes in alkaline water electrolysers. A recent paper [24] has described the application of NiAl coatings prepared by PVD and used as cathodes in alkaline water electrolysis.

## Experimental

### *Deposition conditions*

Coatings were deposited using a Teer Coatings Ltd magnetron sputter ion-plating UDP 650 system [25]. Four targets (metal, alloy or compound) could be used during deposition processes. Table 1 shows the alloy target materials used in this work. Argon, or argon plus helium (both 99.999% purity and supplied by BOC Edwards), was used as the working gases. The distance between the target and the substrates was about 150 mm. The substrates could either be static or rotated, passing the targets at a controlled rotation speed of 1–10 rpm.

Nickel mesh (DeXmet Corporation, 4 Ni 6-040, 0.00400 nominal thickness, 0.00600 strand width, 0.04000 long diagonal of the diamond) or stainless steel 316L mesh (DeXmet Corporation, 4SS 5-050, 0.00400 nominal thickness, 0.00500 strand width, 0.05000 long diagonal of the diamond) were used as substrates for the cathode and anode electrodes respectively. 316L stainless steel (ASTM A240) and M42 hardened high speed tool steel (ASTM A600, RHC 65 ± 1) flat test pieces were used as witness samples for thickness measurement and adhesion tests. Si wafer pieces were used as substrates for scanning electron microscope (SEM) analyses.

The substrates were cleaned with acetone for 15 min immersed in an ultrasonic bath before drying and mounting into deposition chamber. The chamber pressure before deposition was less than $3.0 \times 10^{-5}$ Torr ($4.0 \times 10^{-3}$ Pa). The substrates were plasma-ion-cleaned prior to deposition for 15 min, under an argon pressure of $3.0 \times 10^{-3}$ Torr (0.4 Pa), and an average approximately −400 V substrate bias from a pulsed direct current (DC) power supply of 250 kHz pulse frequency and 500 ns pulse duration.

HSACs were deposited as a single layer or on top of a smooth dense layer, i.e. a dense under-layer was first deposited via a conventional sputtering processes, with argon as the working gas at a pressure of ~0.4 Pa (~3 mTorr) and −35 ~ −55 V substrate bias. HSACs were deposited at a relatively high deposition pressure of 10.0 Pa (75.0 mTorr) achieved by adjusting the throttle valve of the pumping system, with an Ar and He mixture as the working gas (Ar/He flow ratio = 1:2), a type I unbalanced magnetron [15,26] and a negative self-bias from the floating potential of the substrates. Pt, Ni, Mo (all 99.5% purity), 316L stainless steel, Monel alloy 400, and Hastelloy C276, C22 and B3 (all industrial grade) were used as sputtering targets. The metal or alloy target was connected to a DC power supply and a current of 5.5 A was applied during deposition processes. The thickness of the coatings was controlled by changing the duration of the deposition. No additional heating was applied during deposition process and the substrate temperature remained below 473 K.

### *Thickness measurement*

Coating thickness was assessed using a ball crater taper cross-section method (ASTM E1182-93) on coatings deposited on steel substrates. Three measurements were taken for each sample and the average values are reported.

Please cite this article in press as: Zhang X, et al., High surface area coatings for hydrogen evolution cathodes prepared by magnetron sputtering, International Journal of Hydrogen Energy (2015), http://dx.doi.org/10.1016/j.ijhydene.2014.12.107

### Coating adhesion testing

The adhesion of the coatings was measured with a Teer ST3001 scratch/wear tester using a Rockwell diamond tip sliding against the coating with a load increasing by 100 N $min^{-1}$ from 10 to 100 N at a sliding speed of 10 mm $min^{-1}$. The scratch critical load *Lc* of the coating was determined by visual observation in an optical microscope and defined as the point at which coating delamination was first observed either in or at the edge of the scratch track (ASTM C1624-05). A conventional Rockwell indentation test under a load of 150 kgf, was also used as an indication of adhesion [27].

### Scanning electron microscopy (SEM)

The morphology of the coated samples was examined using a JEOL 7000 field emission gun SEM. Coated samples were fractured for cross-sectional SEM observation. The composition and elemental distributions of the coatings were investigated using a SAMX Energy Dispersive X-Ray Analyser (EDX) system, which was attached to a Cambridge Instruments Stereoscan 200 SEM.

### Electrochemical measurements

Electrochemical measurements were carried out using an Autolab potentiostat/galvanostat PGSTAT30 in a small undivided beaker cell (volume 20 $cm^3$) equipped with a water jacket connected to a Camlab W14 water thermostat. Cyclic voltammetry measurement was used to evaluate the electrochemically active surface areas of coated and uncoated electrodes. Cyclic voltammetry for platinum coating was conducted in 1 M $H_2SO_4$ *vs* saturated calomel reference electrode while nickel coating was in 1 M NaOH *vs* Hg/HgO reference electrode.

Slow scan voltammetry into the potential region for $H_2$ evolution has been used to compare the catalytic activities of the coating materials. A small piece of coated mesh, a large area of platinum gauze and a mercury/mercury oxide

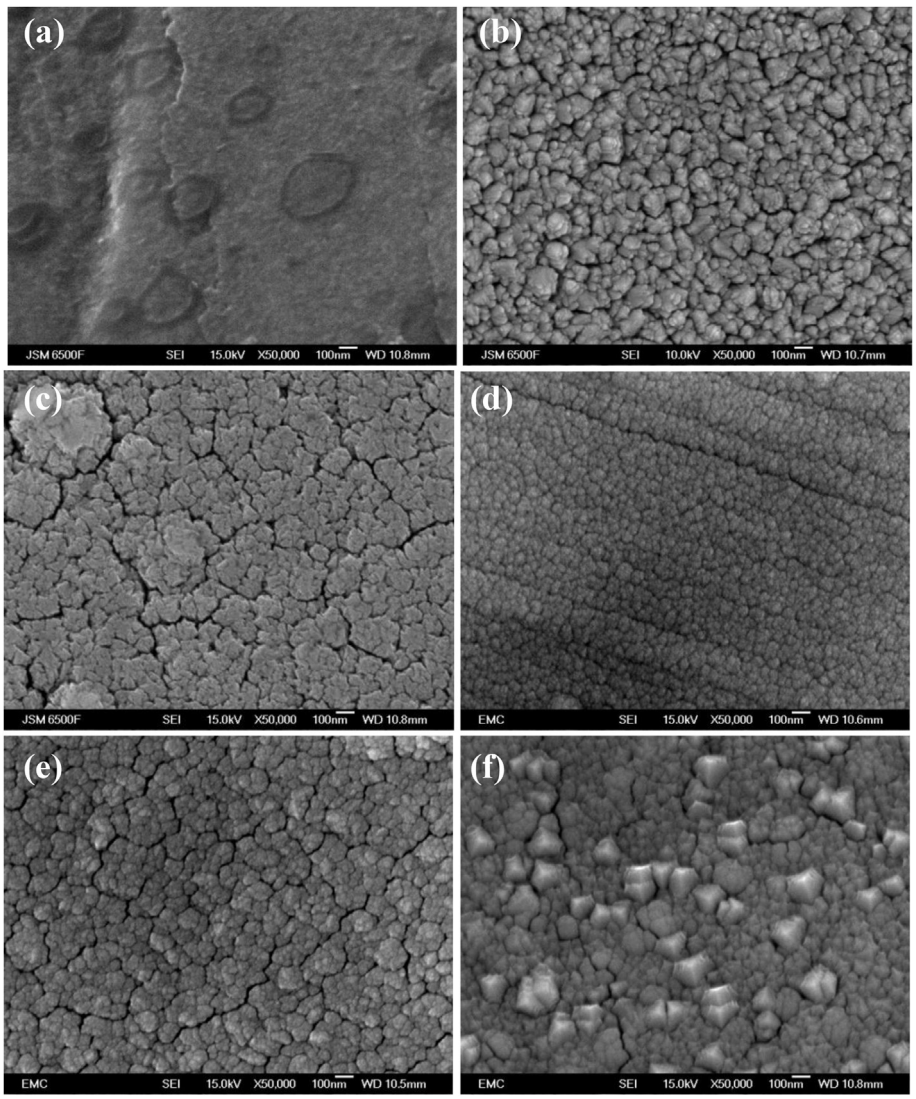


**Fig. 1 – SEM images of (a) an uncoated Ni mesh and the coatings produced by magnetron sputtering in the conditions developed for high surface area deposits (b) Pt (c) Ni (d) NiMo (e) Monel 400 (f) stainless steel 316. Magnification ×50,000.**

Please cite this article in press as: Zhang X, et al., High surface area coatings for hydrogen evolution cathodes prepared by magnetron sputtering, International Journal of Hydrogen Energy (2015), http://dx.doi.org/10.1016/j.ijhydene.2014.12.107

electrode (Hg/HgO in 4 M NaOH) were used as working, counter and reference electrodes, respectively. The reference electrode was always at the same temperature as the working electrode.

The electrolyses were carried out at a temperature of 333 K using an alkaline solid polymer electrolyte (SPE) water electrolysis cell with a 160 μm thick, hydroxide ion conducting membrane under development by ITM Power plc, UK. The cell was assembled with the two mesh electrodes (each geometric area, 9 $cm^2$) pressed up against the membrane and 4 M NaOH flowed down the rear of the meshes at a flow rate of 15 $cm^3\ min^{-1}$ to prevent gas accumulation. The anode was the fine stainless steel mesh coated with a Ni/Fe hydroxide layer by cathodic electrodeposition [28] and the cathodes were the various coated materials. Prior to recording the cell current versus cell potential curves, electrolysis with a current density of 1 A $cm^{-2}$ for 1 h was carried out in order for the cell components to approach their steady state performance. The longevity tests were carried out in the same cell under constant electrolysis at a current density of 1 A $cm^{-2}$ at 333 K and ambient pressure.

## Results

### *Magnetron sputtering deposition*

Using a single magnetron target, layers deposited included Pt, Ni, steels, monels and hastelloys and using multiple magnetron targets, NiMo alloy. The substrates used were silicon, stainless steel and nickel, in the form of flat surfaces and meshes. Because of the intended application in alkaline water electrolysis, the emphasis was on nickel and steel meshes and a coating thickness of 0.5–5 μm.

A typical preparation procedure, in this case for a high area NiMo deposit onto a stainless steel mesh, illustrates the approach. Firstly a dense NiMo alloy layer was deposited at a low Ar pressure of $3.0 \times 10^{-3}$ Torr (~0.4 Pa), and the NiMo deposits were continuously bombarded under −55 V bias during the deposition processes. The porous NiMo alloy top layer was deposited using a type I unbalanced magnetron [26], at a higher pressure of ~75 mTorr (~10.0 Pa), with a combination of Ar and He as working gas (Ar/He flow ratio = 1:2), and without bias bombardment. These conditions were chosen because the higher the deposition pressure leads to a shorter the mean free path of the sputtered particles, and hence, a greater the opportunity for inelastic collisions in transit to the substrate. The resulting lower mobility of the depositing particles enhances the shadowing effect of sputtered particles emerging from the multidirectional plasma, and results in the deposition of films with a more open structure and a rougher surface [29–31]. Helium is lighter and He atoms have higher average velocities than Ar atoms at a given temperature and pressure. Therefore, the presence of He in the plasma can result in more collisions with the sputtered particles, and results in the formation of clusters in the gas phase. In consequence, the arrival of these larger particles to the surface with lower mobility leads to the deposition of films with a more open structure and a rougher surface morphology [29–31].

Fig. 1 shows the SEM images of the surfaces of a Ni mesh substrate and five high surface area deposits formed under the conditions described above. It can immediately be seen that all the deposits are uniform and have a much increased effective surface area compared to the substrate. They consist of closely packed fine, nano-crystalline features (typically on a ~100 nm scale). Fig. 2 shows a cross-sectional SEM image of a two layer NiMo alloy coating on a Si substrate. The lower, dense layer, thickness ~0.75 μm, is essentially featureless but the upper layer, thickness ~1.3 μm, is clearly porous with columnar features.

The electrochemically active surface areas were explored using cyclic voltammetry. Fig. 3 reports voltammogams for the high surface area platinum and nickel deposits recorded in conditions appropriate for a change in the oxidation state of the metal surfaces. The large current densities for the peaks at both Pt and Ni coatings should be stressed. The Pt response was obtained in 1 M sulphuric acid and it shows the classical peaks for the adsorption/desorption of hydrogen between +100 mV and −300 mV vs SCE as well as the wave for the formation of PtO and a peak for its reduction back to Pt at less positive potentials [32]. The charge under the peaks for hydrogen evolution peaks was used to estimate the real surface area assuming that the charge for the deposition of a monolayer of hydrogen atoms is 210 μC $cm^{-2}$; the roughness factor for this high surface area Pt deposit was estimated to be 244 (see Fig. 3(a), solid line). By comparison, a Pt coating deposited via a conventional sputtering process gave a roughness factor of 10 (see Fig. 3(a), dash line). The voltammogram for Ni was obtained in 1 M NaOH and shows the symmetrical peak for the conversion of the existing surface layer of $Ni(OH)_2$ to NiOOH at +450 mV vs Hg/HgO and the reverse reaction at +315 mV (see Fig. 3(b), solid line) [33]. The charges under these peaks led to a roughness factor of 239. A similar experiment with the uncoated Ni substrate led to a roughness factor of 6 (see Fig. 3(b), dash line). It should also be noted that both cyclic voltammograms in Fig. 3 show unusually sharp features for such high area surfaces and this implies a very uniform current and potential distribution over the surface.

The adhesion of the deposited coatings was examined using both indentation and scratch tests. These are illustrated using a SS316 deposit on a stainless steel substrate in Fig. 4. Fig. 4(a) is the optical image of a Rockwell indentation and no

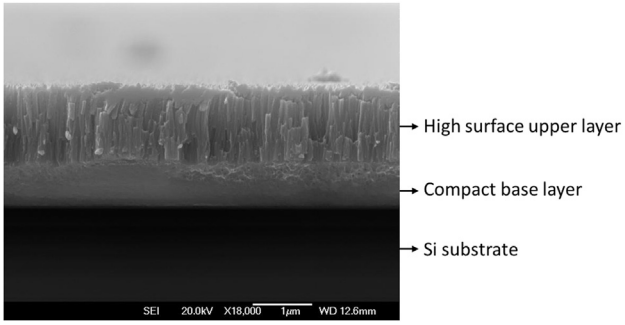


**Fig. 2 – SEM of a cross section of a double layer NiMo coating on a Si substrate. The dense, base layer was deposited in conventional conditions and the porous upper layer in the conditions stated in the text. Magnification ×10,000.**

Please cite this article in press as: Zhang X, et al., High surface area coatings for hydrogen evolution cathodes prepared by magnetron sputtering, International Journal of Hydrogen Energy (2015), http://dx.doi.org/10.1016/j.ijhydene.2014.12.107

flaking or delamination of the coating can be seen at the periphery of the impact area despite the substantial deformation resulting from the impact. Fig. 4(b) shows the scratch test with an increasing load up to a final load of 100 N (at the end of the scratch) and again the damage to the coating along the edge and scratching track is minimal. The adhesion of the coating is excellent. Similar results were obtained with all other coatings tested. It was also found that no visible mechanical damage to the coatings occurred during extensive handling and electrochemical testing.

For four alloys, the composition of the deposits were compared to the composition of the corresponding single magnetron targets, see Table 1, and it can be seen that the composition of the deposits follows closely that of the target. In a further series of depositions using nickel and molybdenum targets, it was shown that the composition of the deposits could be varied between Ni80Mo20 and Ni52Mo48 by controlling the sputtering power applied on the target during depositions. Finally, the compositional uniformity and crystallinity of the coatings was examined using EDAX elemental mapping and XRD respectively. Fig. 5 shows EDAX elemental mapping (a) and XRD spectrum (b) for the Ni–Fe–Cr alloy coating. It can be seen that the coating is very uniform and shows highly ordered crystalline formation.

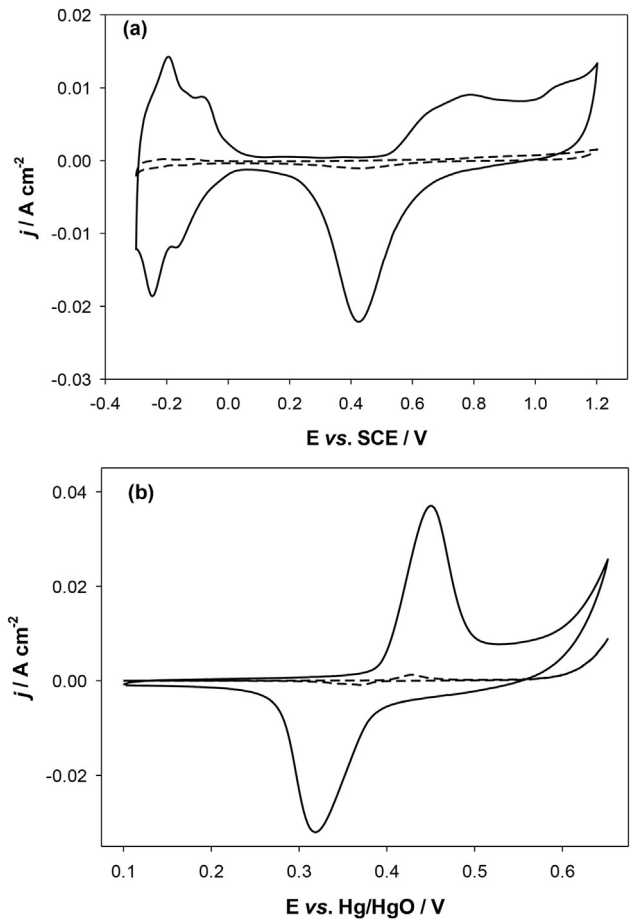


**Fig. 3 – Cyclic voltammograms recorded at (a) a Pt coating electrode in 1 M $H_2SO_4$ at 293 K (solid line: high surface area Pt; dash line: Pt coating via a conventional sputtering process) and (b) a nickel coating electrode in 1 M NaOH at 293 K (solid line: high surface area Ni; dash line: uncoated Ni). Potential sweep rate: 50 mV $s^{-1}$.**

### *Studies of deposits as hydrogen evolution cathodes*

Fig. 6 reports polarisation curves recorded with a potential scan rate of 1 mV $s^{-1}$ for uncoated nickel mesh and selected high surface materials prepared on nickel mesh as described in the previous section; the figure shows data for high surface area Ni and NiMo alloy together with high surface area Pt for comparison. The electrolyte is 4 M NaOH at a temperature of 333 K, similar to the conditions used in commercial water electrolysers, and the current density range is also chosen to be that of interest for water electrolysis. The slight scatter in the data results from the high rate of hydrogen bubble formation and release from the cathode surface. It can be seen that the use of the high surface area cathodes leads to a large shift in the responses to less negative potentials corresponding to a decrease in overpotential for hydrogen evolution and to an expected decrease in energy consumption when high area cathodes are employed in a water electrolyser. Moreover, consistent with the literature [3,34], alloying the nickel with molybdenum leads to a further decrease in the overpotential for $H_2$ evolution; a current density of 0.1 A $cm^{-2}$ can be achieved at −980 mV vs Hg/HgO and 1.0 A $cm^{-2}$ at −1230 mV vs Hg/HgO. The improved performance of the NiMo alloy is thought to result from partial dissolution of the molybdenum from the surface into the alkaline electrolyte, further increasing the surface area. In fact, the performance of the high surface area NiMo alloy is close to that of high surface area platinum and the use of the alloy rather than platinum as the cathode in a water electrolyser corresponds to a substantial cost reduction. In a further set of experiments, polarisation curves were recorded for a series of NiMo alloys where the % Mo was varied between 20% and 48% but the overpotentials found did not vary significantly. It was also shown that when the alloys were deposited using conventional sputtering conditions so that a smooth deposit was obtained, the same decrease in $H_2$ overpotential decrease was not observed. The influence of deposit thickness was probed by recording polarisation curves for cathodes with deposit thicknesses of 0.5 μm, 1 μm and 2 μm (prepared using different deposition times). With the thinnest coating, the overpotential was higher but above 1.0 μm there was no significant improvement in performance.

The high surface area cathodes were tested in an alkaline SPE water electrolyser presently under development. In the cell configuration used here, the cathode (including uncoated Ni mesh, the coated Ni, NiMo and Pt) and a nickel mesh anode coated with a nickel/iron hydroxide [28] are pressed on either side of a hydroxide permeable membrane with both electrodes fed with 4 M NaOH at 333 K. Fig. 7 shows plots of cell current density versus cell voltage for the alkaline SPE water electrolysis cell with four different cathodes. Again, the advantage of the high surface area cathodes is clear. The high surface area Ni decreases the cell voltage by ~100 mV at a current density of 1.0 A $cm^{-2}$ compared to the uncoated cathode. As expected, the NiMo coating performs significantly better and the cell voltage is 2.04 V at 1.0 A $cm^{-2}$. It outperforms the high area Pt at even

Please cite this article in press as: Zhang X, et al., High surface area coatings for hydrogen evolution cathodes prepared by magnetron sputtering, International Journal of Hydrogen Energy (2015), http://dx.doi.org/10.1016/j.ijhydene.2014.12.107

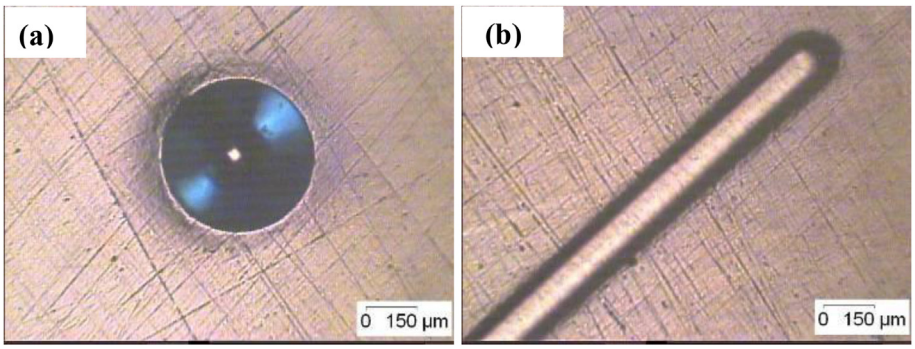


**Fig. 4 – (a) Rockwell indent test under load of 150 kgf and (b) standard scratch test with load up to 100 N for a high surface area stainless steel coating on M42 steel.**

higher current density. Fig. 8 illustrates the stability of performance for the zero gap cells by showing the cell voltage with a current density of 1 A $cm^{-2}$ as a function of time for the same four cathodes. It is evident that the cell voltages show a small increase at a very early stage of operation and then settle down to a stable value. Once more, the reduced cell potential, and hence energy consumption, with the high surface area cathodes is evident. In this test, the high surface area NiMo is the best performing material, giving a cell voltage of 2.14 V. The data in Fig. 8 is limited to an electrolysis time of 2 days but, in fact, the electrolysis with the NiMo cathode was continued for 10 days without any increase in cell voltage. Even after 10 days there was no visible change to the appearance of the NiMo deposit [34].

## Discussion

By using a type I unbalanced magnetron, a mixture of Ar and He as the working gas, a higher pressure and the absence of bias bombardment, it is possible to employ magnetron sputtering for deposition of high surface area coatings. Roughness factors of ~240 have been demonstrated. Using a single target,

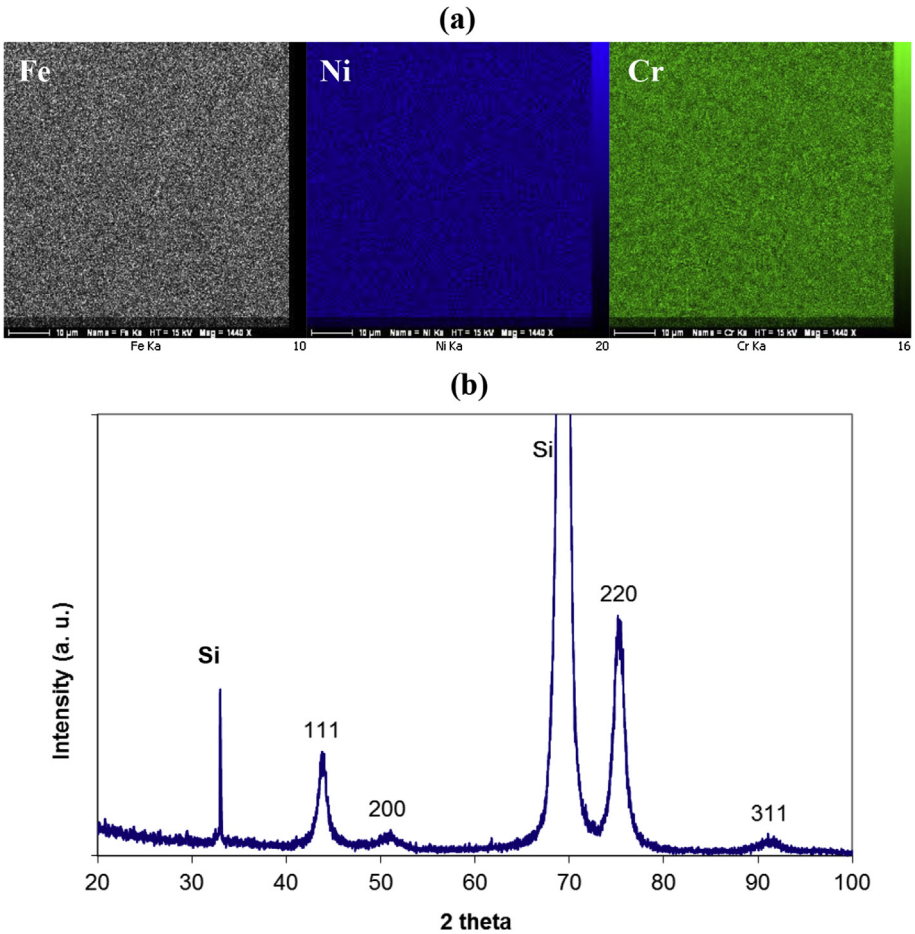


**Fig. 5 – (a) EDAX elemental maps and (b) XRD spectrum for the coating of a Ni–Fe–Cr alloy on a silicon substrate.**

Please cite this article in press as: Zhang X, et al., High surface area coatings for hydrogen evolution cathodes prepared by magnetron sputtering, International Journal of Hydrogen Energy (2015), http://dx.doi.org/10.1016/j.ijhydene.2014.12.107

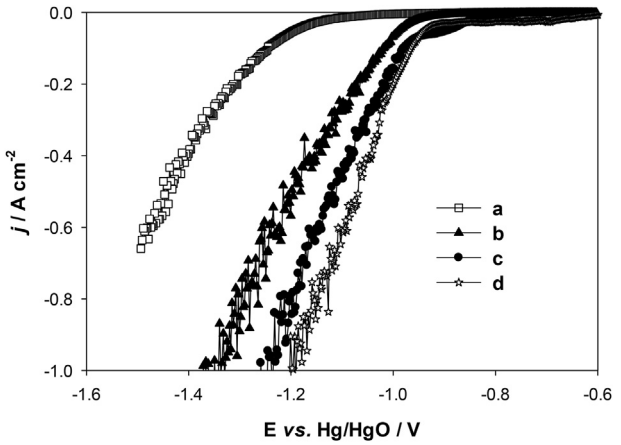


**Fig. 6 – Plots of current density vs potential for (a) uncoated Ni mesh and Ni mesh coated with (b) high area Ni (c) high surface area Ni80Mo20 and (d) high area Pt. Electrolyte: 4 M NaOH. Temperature: 333 K. Potential scan rate: 1 mV $s^{-1}$.**

a wide range of metals (e.g. Ni, Pt) and alloys (e.g. steels, monels and hastelloys) can be deposited in high area form and using multi-targets, alloys (e.g. NiMo) of controlled composition may be deposited in high area form. The layers consist of closely packed, fine, nano-crystalline features (typically with dimensions of ~100 nm). They have excellent adhesion and uniformity and are robust during extensive handling and use. Their thickness is easily varied in a controlled manner between a few nm and several microns. It is also possible to deposit multiple layers of different composition and/or structure. In this work, the most successful coatings consisted of a dense under-layer for corrosion protection with a porous top layer with a high surface area to promote high rate hydrogen evolution at low overpotential.

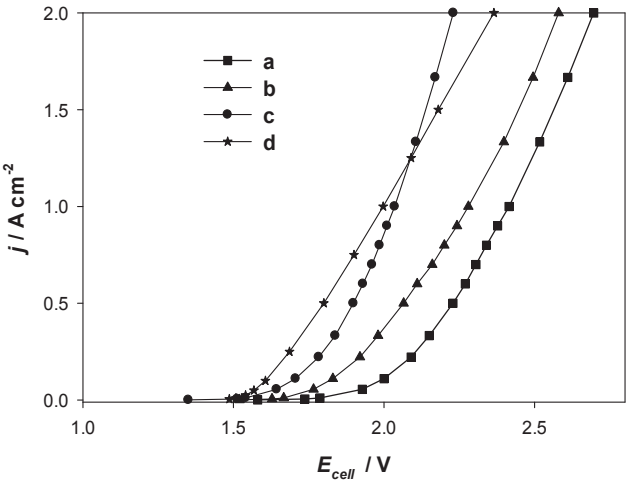


**Fig. 7 – Current density *vs* cell voltage plots for 4 cells with different cathodes (a) uncoated Ni mesh and Ni mesh coated with (b) high area Ni (c) high area Ni80/Mo20 and (d) high area Pt. In each case the cell has a zero gap configuration with an $OH^-$ conducting membrane and an anode of Ni mesh coated with a NiFe hydroxide. 4 M NaOH feeds to both electrodes. Temperature 333 K.**

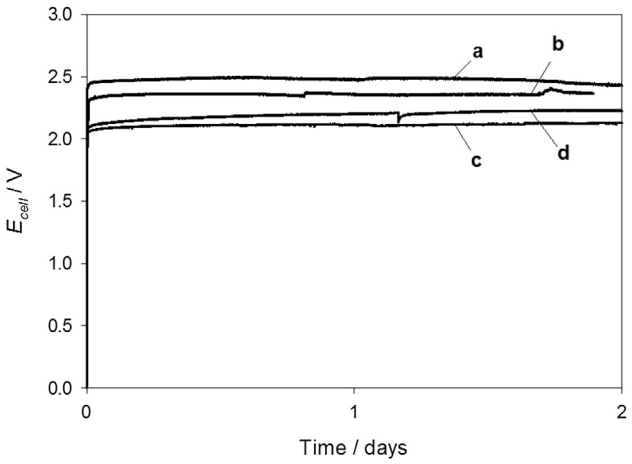


**Fig. 8 – Cell voltage vs time plots for 4 zero gap cells with different cathodes (a) uncoated Ni mesh and Ni mesh coated with (b) high area Ni (c) high area Ni80/Mo20 and (d) high area Pt. In each case the cell has a zero gap configuration with an $OH^-$ conducting membrane and an anode of Ni mesh coated with a NiFe hydroxide. 4 M NaOH feeds to both electrodes. Temperature 333 K. Current density 1 A $cm^{-2}$.**

All the high surface area deposits enabled the evolution of hydrogen at high rates in alkaline media, i.e. support current densities >1 A $cm^{-2}$, and this was achieved at significantly lower overpotential than that of the uncoated nickel. For the alkaline water electrolyser, the preferred coating was a NiMo alloy. It gave overpotentials for hydrogen evolution comparable to those from high surface area platinum. When tested in a zero gap, alkaline water electrolyser, the NoMo alloy cathode performed excellently and the electrolysis cell had lower energy consumption. It allowed continued operation with a current density of 1 A $cm^{-2}$ with a cell voltage of 2.14 V; this cell voltage did not increase even after 10 days. These NiMo coatings on nickel or steel are realistic alternatives to precious metal coated cathodes and could be an important component in future, low cost water electrolysers.

The concept of increasing the rate of electrocatalytic reactions by increasing the real surface area of the electrode is, of course, general, applying for example to oxygen and chlorine evolution. Indeed, preliminary results show that the coatings fabricated by the modified magnetron sputtering technique give substantially reduced overpotentials for $O_2$ evolution and electrolysis cells with two electrodes produced by this technique give further reductions in cell voltage and energy consumption.

## Conclusions

A novel magnetron sputtering technique has been developed to deposit thin film coatings with significantly increased surface areas. Metallic or compound, high surface area cathodes (HSACs) can be deposited as a single layer or on top of a smooth dense layer, and as multilayers. The thickness of the coatings can be controlled from several nm to several

Please cite this article in press as: Zhang X, et al., High surface area coatings for hydrogen evolution cathodes prepared by magnetron sputtering, International Journal of Hydrogen Energy (2015), http://dx.doi.org/10.1016/j.ijhydene.2014.12.107

microns, with excellent adhesion and uniformity. The optimised thickness of catalytic HSACs for alkaline zero gap water electrolyser was found to be about 1.0–1.5 μm.

Compared with uncoated nickel mesh, although a significant reduction in the electrochemical cell potential was achieved with magnetron sputtered pure Ni-HSACs, an even lower potential and improved stability were demonstrated for a NiMo-HSAC, which was found to be one of the best nickel alloy coating candidates. NiMo-HSAC by magnetron sputtering was shown to be a stable coating that can support very high current densities in alkaline media. A decrease in the cell voltage of >200 mV was achieved, in alkaline SPE water electrolysis tests at a current density of 1 A $cm^{-2}$ tested at 333 K and at ambient pressure. The cathode HSACs reported here are of potential importance for use as low cost non-precious metal catalysts in alkaline electrolysis.

## Acknowledgement

The authors acknowledge financial support from the UK Technology Strategy Board (project number: TP200089). They are also grateful to Dr X. Li (University of Birmingham) for some of the SEM analyses.

## REFERENCES

[1] Pletcher D, Walsh FC. Industrial electrochemistry. Chapman and Hall; 1991.
[2] Plzak V, Rohland B, Wendt H. In: White RE, Bockris JO'M, Conway BE, editors. Modern aspects of electrochemistry, vol. 26. Plenum; 1994.
[3] Trasatti S. Progress in cathode activation. In: Gerischer H, Tobias CW, editors. Advances in electrochemical science and engineering, vol. 2. VCH; 1992. p. 1–85.
[4] Zeng K, Zhang D. Recent progress in alkaline water electrolysis for hydrogen production and applications. Prog Energy Combust Sci 2010;36:307–26.
[5] Grigoriev SA, Porembskii VI, Fateev VN. Pure hydrogen production by PEM electrolysis for hydrogen energy. Int J Hydrogen Energy 2006;31:171.
[6] Pletcher D, Li X. Prospects for alkaline, zero gap water electrolysers for hydrogen production. Int J Hydrogen Energy 2011;36:15089–104.
[7] Damian A, Omanovic S. Ni and Ni Mo hydrogen evolution electrocatalysts electrodeposited in a polyaniline matrix. J Power Sources 2006;158:464–76.
[8] Panek J, Budniok A. Ni + Mo composite coatings for hydrogen evolution reaction. Surf Interface Anal 2008;40:237–41.
[9] Henrique dos Santos Andrade M, Lima Acioli M, Ginaldo da Silva Junior J, Pereira Silva JC, Oliveira Vilar E. Preliminary investigation of some commercial alloys for hydrogen evolution in alkaline water electrolysis. Int J Hydrogen Energy 2004;29:235–41.
[10] Hu W, Cao X, Wang F, Zhang Y. A novel cathode for alkaline water electrolysis. Int J Hydrogen Energy 1997;22:441–3.
[11] Olivares-Ramírez JM, Campos-Cornelio ML, Uribe Godínez J, Borja-Arco E, Castellanos RH. Studies on the hydrogen evolution reaction on different stainless steels. Int J Hydrogen Energy 2007;32:3170–3.
[12] Rosalbino F, Maccio D, Angelini E, Saccone A, Delfino S. Characterization of Fe-Zn-R (R = rare earth metal) crystalline alloys as electrocatalysts for hydrogen evolution. Int J Hydrogen Energy 2008;33:2660–7.
[13] Mattox DM. Handbook of physical vapour deposition (PVD) processing. 2nd ed. Springer; 2010, ISBN 0815520379.
[14] Colligon J. Ion assisted sputter deposition. Phil Trans R Soc 2004;362:103–6.
[15] Mathews A. Plasma-based physical vapour deposition surface engineering processes. J Vac Sci Technol A 2003;21:S224–31. http://dx.doi.org/10.1116/1.1599893.
[16] Kelly PJ, Arnell RD. Magnetron sputtering: a review of recent developments and applications. Vacuum 2000;56:159–72.
[17] Kelly PJ, O'Brien J, Arnell RD. The production of porous and chemically reactive coatings by magnetron sputtering. Vacuum 2004;74:1–10.
[18] Dunnill ChW, Parkin IP. Nitrogen-doped $TiO_2$ thin films: photocatalytic applications for healthcare environments. Dalton Trans 2011;40:1635–40.
[19] Skorb EV, Antonouskaya LI, Belyasova NA, Shchukin DG, Mőhwald H, Sviridov DV. Antibacterial activity of thin-film photocatalysts based on metal-modified $TiO_2$ and $TiO_2$:$In_2O_3$ nanocomposite. Appl Catal B 2008;84:94–9.
[20] Maneerat C, Hayata Y. Antifungal activity of $TiO_2$ photocatalysis against *Penicillium expansum* in vitro and in fruit tests. Int J Food Microbiol 2006;107:99–103.
[21] Caillard A. Deposition and diffusion of platinum nanoparticles in porous carbon assisted by plasma sputtering. Surf Coat Technol 2005;200:391–4.
[22] Zhang X, Cooke K, Carmichael P, Parkin IP. The deposition of crystallized $TiO_2$ coatings by closed field unbalanced magnetron sputter ion plating. Surf Coat Technol 2013;236:290–5.
[23] WO2013124647 A3. High surface area (HSA) coatings and method for forming the same. Oct 16th 2013.
[24] Kjartansdottir CK, Nielsen LP, Møller P. Development of durable and efficient electrodes for large-scale alkaline water electrolysis. Int J Hydrogen Energy 2013;38:8221–31.
[25] Laing K, Hampshire J, Teer D, Chester G. The effect of ion current density on the adhesion and structure of coatings deposited by magnetron sputter ion plating. Surf Coat Technol 1999;112:177–80.
[26] Savvides N, Window B. Unbalanced magnetron ion-assisted deposition and property modification of thin films. J Vac Sci Technol A 1986;4:504–8.
[27] Daimler-Benz Rockwell-C adhesion test, Vereim Deutscher Inbenieure, *VDI-Richtlinie* 3198 (*HRC adhesive test*). Koln: Beuth Verlag; 1993.
[28] Li X, Walsh FC, Pletcher D. Nickel based electrocatalysts for oxygen evolution in high current density alkaline water electrolysers. Phys Chem Chem Phys 2011;13:1162–7.
[29] Salinga C, Kappertz O, Wuttig M. Reactive direct current magnetron sputtering of tungsten oxide: a correlation between film properties and deposition pressure. Thin Solid Films 2006;515:2760–4.
[30] Yoo SJ, Choa YH, Park HS, Lee JK, Sunga YE. High utilization of Pt nanocatalysts fabricated using a high-pressure sputtering technique. J Power Sources 2008;178:547–53.
[31] Jankowski AF, Hayes JP. Sputter deposition of a sponge like morphology in metal coatings. J Vac Sci Technol A 2003;21:422–5. http://dx.doi.org/10.1116/1.1545759.
[32] Bai L, Gao L, Conway BE. Problem of in situ real-area determination in evaluation of performance of rough or porous, gas-evolving electrocatalysts. J Chem Soc Faraday Trans 1993;89:235–42.
[33] Fleischmann M, Korinek K, Pletcher D. Oxidation of organic compounds at a nickel anode in alkaline solution. J Electroanal Chem 1971;31:39–49.
[34] Pletcher D, Li X, Wang S. A comparison of cathodes for zero gap alkaline water electrolysers. Int J Hydrogen Energy 2012;37:7429–35.

Please cite this article in press as: Zhang X, et al., High surface area coatings for hydrogen evolution cathodes prepared by magnetron sputtering, International Journal of Hydrogen Energy (2015), http://dx.doi.org/10.1016/j.ijhydene.2014.12.107